

Properties of a New PrimePACK™ IGBT Module Concept for Optimized Electrical and Thermal Interconnection to a Modern Converter Environment

O. Schilling, M. Wölz, G. Borghoff, Th. Nübel, G. Bräker, Chr. Lübke,
eupec GmbH , Warstein

Abstract:

We present a new power module concept that is specifically optimized for the integration in a modern converter. The most important benefits are improved thermal properties, a low stray inductance and an advantageous interface to both driver board and load circuitry. Studies on the device performance are presented based on measurements and numerical simulations.

I Introduction

IGBTs have made their way into many applications and from the beginning the development of housing concepts has been pursued in parallel to the progressive evolution of silicon IGBTs and diodes. The housing has to meet both mechanical, electrical and thermal requirements in order to form a proper interface between the silicon chips and the converter surroundings. Very established designs are for example half-bridge and single-switch modules with 62mm width of the baseplate or the IHM standard that evolved in 1993 (1) and is employed under industrial and rolling stock conditions. The Econo based housing-principle (2) is characterized by its flat geometry and the higher degree of integration with up to three phase legs in one module. The concept has been further developed leading into the EconoPACK™+ standard in 2000 (3). Besides also packaging concepts without baseplates are available for example SkiIP® modules or the LoPAK / SkiM® concept. Other housings that have achieved a worldwide acceptance are listed in a standard (4). In this work a new concept for a power module is presented that offers flexibility, fulfils economical requirements and that is adapted to the needs of state of the art IGBT chip technology with high current density. In the following we first present the outline and the main data of the PrimePACK™ concept. In the succeeding parts of this work we go through its thermal, electrical and mechanical characteristics.

II PrimePACK™ module line-up

The following tabular summary gives the range of types that is realised within the PrimePACK™ line-up being based on 1200V and 1700V IGBT3/Emcon3 chip technology (5,6). The current range from 400A...1200A (1200V) or 400A...900A (1700V) is covered by two module sizes. The rating is referring to the electrical configuration of a half bridge, thus the totally installed current is twice as high. PrimePACK™ power modules thus are suitable for the medium power range for converters driving up to 540kW for housing 1 or 800kW if the larger housing 2 type is concerned.

VCES=1200V, Halfbridge		
IC [A]	Housing 1	Housing 2
400	FF400R12IE3	
600	FF600R12IE3	
800	FF800R12IE3	
900		FF900R12IE3
1200		FF1200R12IE3

VCES=1700V, Halfbridge		
IC [A]	Housing 1	Housing 2
400	FF400R17IE3	
500	FF500R17IE3	
600	FF600R17IE3	
750		FF750R17IE3
900		FF900R17IE3

Table 1: PrimePACK™ module line-up for 1200V and 1700V.

Figure 1 contains a sketch of the two new housings. The footprint exhibits a rectangular shape. There is a baseplate that can be tightly fitted on the heatsink by screws in close distance. The module height is ~38mm in accordance with the height of the worldwide established IHM-type. On top of the module the DC (+/-) and phase-output load terminals can be attached to an inverter busbar by M8 screws securing a reliable joint with a large contact area. The driver board can be mounted on a separate plateau at the front side of the PrimePACK™.

The plateau is significantly lower compared to the level of the load terminals thus enabling a busbar to be guided above the driver board. The mechanical and electrical attachment of the driver PCB is done by M4 screws that guarantee both safe contact even under rough conditions like mechanical vibration and furthermore the possibility to remove the PCB again e.g. for maintenance purpose.



Fig. 1: mechanical outline of housing 1 (left) and housing 2 (right) PrimePACK™. Both types form a halfbridge configuration with 3 connections: DC+, DC- and phase output.

III Thermal properties and usability

The thermal properties of the PrimePACK™ concept result from the design of the footprint and the internal chip arrangement enabling:

- a) improved spreading of the heat generated in the silicon into the baseplate and into the heatsink,
- b) strong thermal contact between baseplate and heatsink.

The ability to spread heat and avoid hot spots due to high power concentration is markedly influenced by the parameter $Q = A_{bp} / A_{Si, total}$, the ratio between baseplate area A_{bp} and the total area of installed silicon $A_{Si, tot}$. The outline of the PrimePACK™ is resulting in a Q-value of about 6 if the module with the highest current rating and highest possible installed total chip area is regarded. Many other state of the art power modules reach Q-values of about 4 if the evaluation is done under comparable terms. Therefore the area that is at disposal to dissipate the losses into the heatsink is enlarged by roughly 50% in comparison to many existing designs.

A further important aspect is the homogeneity of heat density across the baseplate. The schematic sketch in figure 2 shows how this target is reached by the PrimePACK™: It

presents a FEM simulation of the temperature distribution inside a PrimePACK™ module for motor operation. IGBT- and diode chips that are acting as centres for heat generation are distributed along the total length of the device. The dissipated heat is 155W per IGBT chip and 31W per diode chip, a typical ratio for motor operation. The dissipated power is leading to $T_{vj, max} = 125^\circ C$ if the assembly is mounted on a watercooled heatsink with $T_a = 60^\circ C$. The alternating sequence of IGBTs and diodes is beneficial if the circumstance is taken into account that the losses are primarily produced in only one type of chip (either only IGBTs or only diodes), a condition that occurs for example in purely motor- or generative operation of an inverter. Finally the arrangement of the two arms of the comprised half-bridge is done in a way that the Si-dies of each individual arm of the half bridge are also distributed along the total area of the baseplate. In order to illustrate this feature the IGBTs in the high side (low side) arm are labelled by "+" ("−") in figure 2. Under normal switching conditions both arms of a half bridge contribute equal amounts of power loss. There are special drive conditions where heat is generated only in one arm of a half bridge for several ms e.g. in servo applications utilising "0 frequency" switching. The arrangement shown in figure 2 is advantageous also for this type of inverter operation.

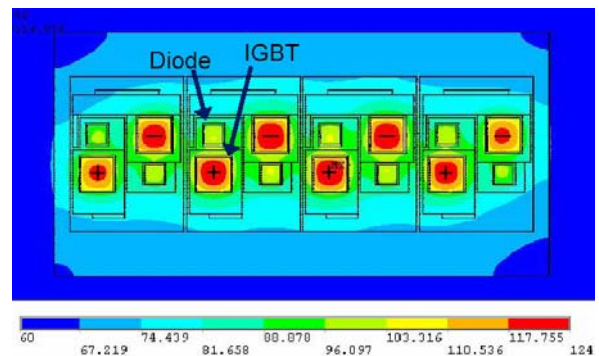


Fig. 2: Schematic top view on a PrimePACK™ baseplate of housing 1 including substrates and the position of IGBT and diode dies. Dies belonging to the upper (lower) arm of the phase leg are denoted "+" ("−"). Colours: FEM simulation of temperature for motor operation.

The second aspect referred to above (b) is concerning the thermal resistance R_{thch} between baseplate and heatsink. In the direction perpendicular to the longitudinal module axis a short distance between baseplate screws of merely ~75mm is realised. In this way the metal surfaces of baseplate and heatsink can be

tightly pressed onto another at the location of the silicon dies. A mechanical analysis of the influence of the screw distance on the force pressing the centre of the baseplate against the heatsink is done based on the following assumptions (see figure 3): the mechanical bow of the baseplate itself prior to mounting is kept constant at $+50\mu\text{m}$. The spacing between the screws is varied in the direction that is effective for the vertical force at the location of the substrates. As a result the correlation in the diagram of figure 3 is obtained: In comparison to a standard 62mm module the contact pressing force is doubled. Taking the above result into account we are aiming at recommending a thermal grease thickness of merely $50\mu\text{m}$ to form an interface with low thermal resistance between power module and cooler. Under the simplified supposition of homogenous heat distribution and a thermal conductivity of $\lambda=1\text{W/m}\cdot\text{K}$ for the thermal grease this is leading to $R_{\text{thch}} = 3.5\text{K/kW}$ for the housing 1 PrimePACK™ (2,4K/kW for the longer version respectively).

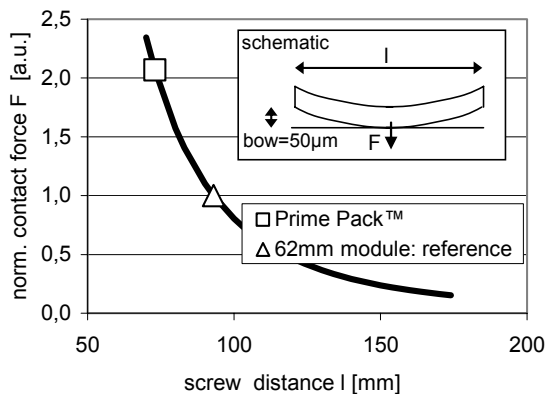


Fig. 3: Force by which the baseplate is pressed against the heatsink as a function of screw distance; inset: cross section of a baseplate: schematic model that is employed for the calculation.

The thermal properties and the effectiveness of a specific module design can be summarized by evaluating the inverter current I_{rms} that can be controlled by a module without exceeding the thermal limit $T_{\text{vj,opmax}}=125^\circ\text{C}$ of the installed Si dies. The calculation is done by IPOSIM (7) that takes into consideration a sinusoidal output current waveform. The following assumptions serve as basis for the calculations:

- IGBT3/Emcon3 silicon is regarded in order to assess the losses,
- Inverter boundary conditions are set: $V_{\text{DC}}=900\text{V}$ and 600V (for 1700V and 1200V

PrimePACK™), $f_0=50\text{Hz}$, $f_{\text{sw}}=1000\text{Hz}$ and 2000Hz ,

- Air cooled heatsink is defined with $T_a=40^\circ\text{C}$ (ambient temperature).

In order to find realistic values for the thermal resistance of the heatsink R_{thha} the following universal approach is made:

$$R_{\text{thha}} = \frac{1}{\alpha \cdot A_{\text{eff}}},$$

with A_{eff} , the effective area of the heatsink that contributes to the transfer of heat to the ambient and α , a constant factor that is primarily determined by the design of the fins, the length of the heatsink l_{hs} and the air flow velocity v_{air} . To obtain a common α , we set $l_{\text{hs}}=200\text{mm}$ and $v_{\text{air}}=10\text{m/s}$. For typical fin designs with $\sim 70\text{mm}$ fin length a constant factor $\alpha \sim 1000$ can be deduced from heatsink data (8). Furthermore the general assumption is made that the effective area of the cooler exceeds the baseplate area of the module mounted on top by 50%: $A_{\text{eff}}=1,5 \times A_{\text{bp}}$. R_{thha} values are obtained that match well the experimental data if this procedure is applied to already existing designs.

As a result the maximum rms current that can be switched without exceeding the thermal limit of the silicon is presented in the diagrams of figure 4 – concerning motor operation – and figure 5, where a comparison between motor and generative operation is given.

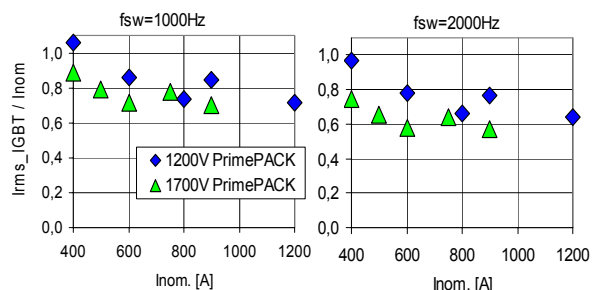


Fig. 4: Ratio between usable rms-inverter current and rated current of module for air cooled heatsink at $T_a=40^\circ\text{C}$, $f_0=50\text{Hz}$, $V_{\text{CC}}=600\text{V}$ (900V respectively) at motor operation.

The overall utilization depends of course strongly on the type of cooling and the switching frequency. For the worst case of air cooled heatsink and a rather high frequency of 2kHz the current that can be driven by the PrimePACK™ ranges between 55...100% of the rated current. At $f_{\text{sw}}=1000\text{Hz}$ the rms current reaches 70%...110% of the rated current. A comparably high utilization is possible because of the

enhanced heat spreading. The usability depends in detail on the degree of filling by silicon dies and can be deduced from figure 4.

Figure 5 proves that the exploitable current differs by less than 10% if the scenarios are regarded that either IGBTs or diodes are acting as primary source of heat generation. This means that the thermal budget is very well aligned to another for both types of devices.

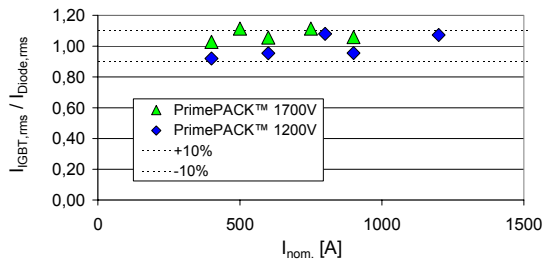


Fig. 5: Ratio between usable IGBT current at motor operation against usable diode current at generative operation. Conditions from fig. 4 with $f_{sw}=2000\text{Hz}$.

IV Electrical features and measurements

A survey is made of the latest demands that result from the behaviour of state of the art silicon technology and from customer feedback concerning the means to control the switching performance of modern devices. As pointed out before, the PrimePACK™ concept is introduced in combination with IGBT3 technology that implies field stop devices and trench gate IGBT cells. Modern silicon devices focus both on a reduction of static losses and switching energies - a target that is achieved by increasing switching speed. This means a higher challenge for control strategies because voltage peaks due to parasitic stray inductance become more pronounced. A number of works point out that additional effort has to be spent in driver development (9,10).

A major requirement therefore is to focus on a low inductive module design that fits into a low inductive circuitry. The most widespread converter concept is based on the 2-level inverter that consists of three half bridge legs that produce output current for three phases. The effective stray inductance is defined by the loop inductance from the DC-link capacitor through one respective halfbridge. The schematic circuitry is given below.

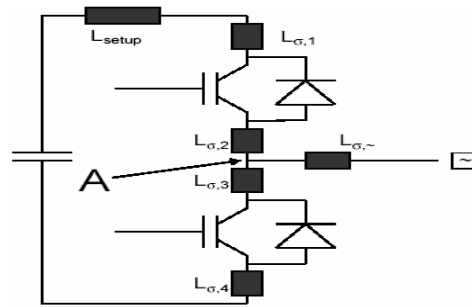


Fig. 6: Schematic of a half bridge including parasitic inductances.

The minimization of parasitic inductance at commutation is achieved by two means in the PrimePACK™ concept.

- The point of commutation (A in fig. 6) is shifted as close to the silicon dies as possible. $L_{\sigma,2}$ and $L_{\sigma,3}$ are reduced to $<1\text{nH}$.
- The inductance of the (+) and (-) contact terminal ($L_{\sigma,1}$ and $L_{\sigma,4}$ in fig. 6) is reduced below 10nH for the housing 2 PrimePACK™ by applying alternating finger shaped terminals. The geometry has been tested by simulation. In the following model (see fig. 7a) a parasitic inductance $L_{\sigma} = 4,06\text{nH}$ is calculated. A corresponding structure with only two terminals of the same clearance (see fig. 7b) exhibits $7,04\text{nH}$.

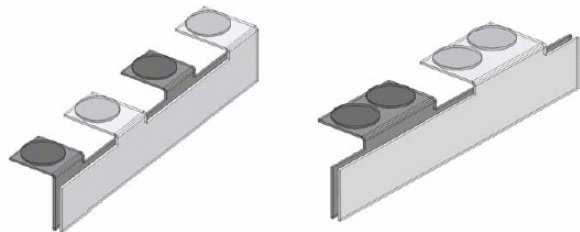


Fig. 7a (left), 7b (right): simplified geometries of +/- terminals used in a 3D simulator to calculate AC-inductance.

Both rules explained above are realized in a first prototype of the housing 2 PrimePACK™. From the measurements done so far, $L_{\sigma} < 10\text{nH}$ is confirmed for one complete phase leg of a halfbridge.

In order to ensure safe switching under a variety of conditions, hard switching investigations are done on a prototype of FF900R17IE3 PrimePACK™. The results are given below. The displayed waveform in figure 8 is a turn-off event at rated current ($I_C=900\text{A}$) and a typical DC-link

voltage $V_{CC}=900V$, which is commonly used in the application of 1700V modules.

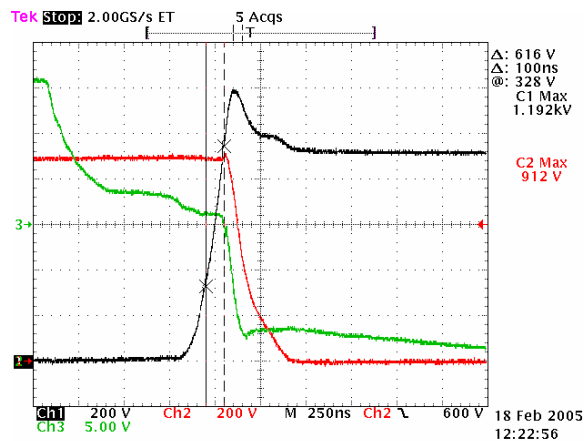


Fig. 8: IGBT turn-off at $T=25^{\circ}C$, $V_{CC}=900V$, $I_C=900A$. DUT is FF900R17IE3 prototype. (Red: I_C , black: V_{CE} , green: V_{GE})

The turn-off curves are smooth and agree with demands resulting from EMC compatibility. The gate resistor is chosen to achieve a high du/dt of $\sim 5kV/\mu s$ which is necessary to limit switching losses. The overvoltage peak is well controlled, does not surpass 1200V and stays safely below the device limit $V_{CES}=1700V$. This also proves the low inductive design characteristic.

The turn-on behaviour has also been studied and an example - also recorded at rated current $I_C=900A$ and $V_{CC}=900V$ - is presented in figure 9: It confirms the smooth switching behaviour and the fact, that the module layout supports the device performance of modern IGBT3 very satisfactorily. Again the gate resistor is chosen to achieve a comparably high di/dt ($\sim 7500A/\mu s$!!), in this way enabling the reduction of turn-on losses and to demonstrate, that safe switching is possible even under extreme conditions.

Finally the PrimePACK™ prototype is strained in a short circuit pulse. The test is also passed and evidence is given in figure 10. The gate voltage is influenced by the rapid change of I_C and V_{CE} and exhibits an overshoot up to 17,5V while I_C climbs up to 6800A peak.

As a conclusion it can be stated that the electrical performance meets the targets set from the beginning. An outstanding feature is the low value of module internal stray inductance. Of course a low inductive inverter design is necessary to profit fully from this device feature.

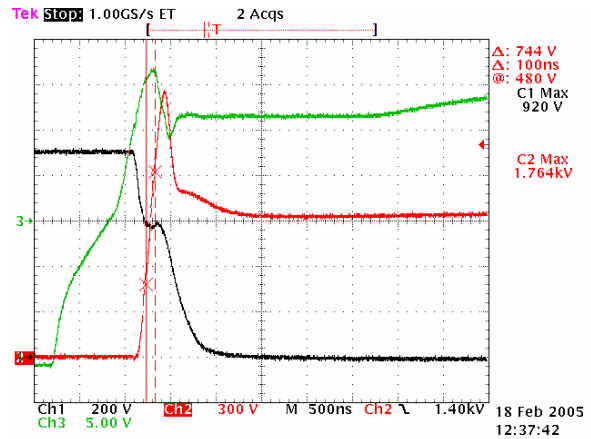


Fig. 9: IGBT turn-on at $T=25^{\circ}C$, $V_{CC}=900V$, $I_C=900A$. DUT is FF900R17IE3 prototype. (Red: I_C , black: V_{CE} , green: V_{GE})

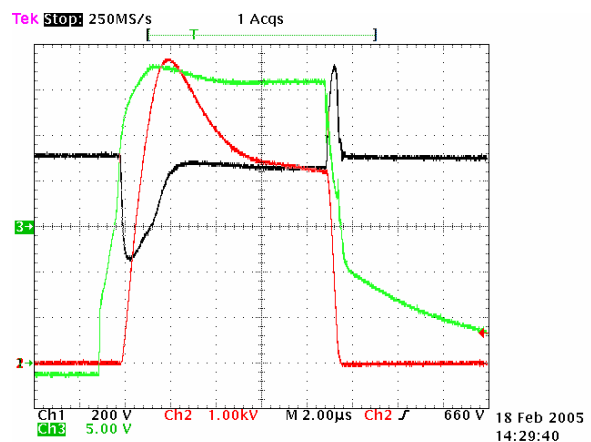


Fig. 10: IGBT short circuit at $T=25^{\circ}C$, $V_{CC}=900V$, DUT is FF900R17IE3 prototype. (Red: I_C , black: V_{CE} , green: V_{GE})

V Integration in a modern converter

A modern converter design has to comply with technical and economical criteria. The new module offers the possibility to utilize the installed current to a high degree and it makes control of fast commutation easy as pointed out in the preceding parts of this work. Furthermore it offers many flexible solutions as far as the connection to the converter busbar and the heatsink of the converter is concerned.

In figure 11 and 12 side views two possible integrations of the PrimePACK™ into a power converter are shown. Figure 11 depicts how the new module can be integrated in a converter if a three layer busbar is preferred for the external electrical load connections. Since the plateau that carries the driver PCB is on a lower level compared to the load terminals of the module a

busbar can be guided above the driver PCB. It depends on the level of DC supply voltage in the load circuit whether an additional insulation on the bottomside of the 3 layer busbar is necessary to ensure safe isolation against the driver

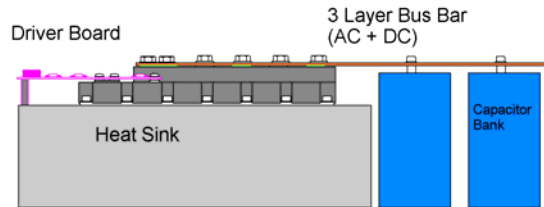


Fig. 11: PrimePACK™ linked to a 3 layer busbar that contains +/- DC and AC load connections.

Multi layer busbars are liable to increase the system costs. An economical solution that employs only a 2 layer busbar is sketched in figure 12. The AC load terminal is excluded from the busbar system and is made of a simple copper connector. The PrimePACK also supports this solution because the AC load terminal of the housing is spatially separated from the +/- DC connectors.

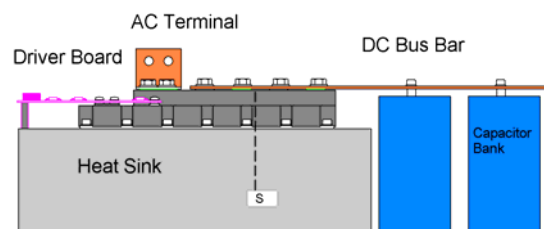


Fig. 12: PrimePACK™ linked to a 2 layer busbar. The AC load terminal is screwed to a separate load connector.

For the sake of clarity the components of the inverter are lined up in one orientation in figure 11 and 12. A further reduction of total stray inductance could be achieved, if the capacitor was orientated at the longside of the IGBT modules.

Finally the PrimePACK™ concept offers a lot of flexibility. The user has the freedom to apply both versions in one inverter design. If the Inverter supports the mounting of the housing 2 - as presented in figure 12 - the housing 1 can be used in the same inverter periphery because the distance between baseplate screws and the position of the load terminal screws is identical

for both types. This is illustrated by the dashed line "S" in figure 12 that indicates the termination of the housing 1 PrimePACK™ if it was used in the same inverter. The application of both PrimePACK™ versions in one inverter family is furthermore simplified, because the geometry and position of the auxiliary terminals on top of both housings stays the same for both types (→ figure 1), which makes it possible to use one driver PCB-geometry for both modules.

VI Conclusion

The PrimePACK™ design is characterized by a slim geometry of the power module. It has advantages both in thermal and electrical respects. It supports enhanced heat spreading inside the module and from the module baseplate to the heatsink and it focuses on a low internal stray inductance of ~10nH for the whole commutation loop if the large version is considered. The housing concept is flexible and offers economical solutions concerning the mechanical integration into a power converter.

References:

- 1) W. Bösterling, H. Ludwig, G. Schulze, M. Tscham, Moderne Leistungshalbleiter in der Stromrichter-technik, Elektrotechnische Zeitschrift etz, Bd. 114 (1993), S. 1310-1319
- 2) M. Feldvoß, G. Müller, A new modular concept of solderable modules simplifies Inverter engineering and logistics
- 3) M. Loddenkötter, M. Münzer, J. Thureau, EconoPACK+ the standard Platform for Modular Inverter Design, Proc. of PCIM, Nuremberg, 2000
- 4) International Standard IEC 60191-2, Mechanical standardization of semiconductor devices – Part 2: dimensions
- 5) M. Hierholzer, Th. Laska, M. Münzer, F. Pfirsch, C. Schäffer, Th. Schmidt, 3rd Generation of 1200V IGBT Modules, Proc. of PCIM, Nuremberg, 1999
- 6) R. Mallwitz, R. Tschirbs, M. Pfaffenlehner, A. Mauder, C. Schäffer, 1700V Trench IGBT Modules, Proc. of PCIM, Nuremberg, 2001
- 7) Dimensioning Programm for loss thermal calculation for eupec IGBT modules, see: www.eupec.com
- 8) Webra datasheet 194-60-15-20
- 9) H:P. Rothwangl, H. Schamböck, Advanced IGBT Control Strategies – Improvement of the Switching Characteristics via Active Gate Control, EPE Toulouse, 2003
- 10) M. Bakran, H.-G. Eckel, M. Helsper, A. Nagel, Challenges in Using the Latest Generation of IGBTs in Traction Converters, EPE Toulouse, 2003